CSIRO PUBLISHING

Marine and Freshwater Research, 2010, **61**, 1268–1277 www.publish.csiro.au/journals/mfr

A novel application of radionuclides for dating sediment cores from sandy, anthropogenically disturbed estuaries

Alexa R. Van Eaton[A,B], *Andrew R. Zimmerman*[A,D], *John M. Jaeger*[A], *Mark Brenner*[A], *William F. Kenney*[A] *and Jeffrey R. Schmid*[C]

[A]Department of Geological Sciences and Land Use and Environmental Change Institute, University of Florida, PO Box 112120, Gainesville, FL 32611, USA.

[B]Present address: School of Geography, Environment and Earth Sciences, Victoria University of Wellington, PO Box 600, Wellington 6012, New Zealand.

[C]Conservancy of Southwest Florida, 1450 Merrihue Drive, Naples, FL 34102, USA.

[D]Corresponding author. Email: azimmer@ufl.edu

Abstract. Reliable sedimentation histories are difficult to obtain in sandy or anthropogenically impacted coastal systems with disturbed sediment profiles and low initial radionuclide activities. This study addresses the problem using radionuclides in sediment cores from Naples Bay estuary, Florida, USA. Non-steady sedimentation and nuclide scavenging processes are shown to limit application of traditional radiometric dating models in this system. Whole-core inventories of excess ^{210}Pb activity ($^{210}Pb_{xs}$) varied from 21 to 96 dpm cm^{-2} among sites, and initial sediment $^{210}Pb_{xs}$ activities were low, decreasing non-uniformly with depth in most cores. Activities of three radioisotopes used for sediment dating (^{226}Ra, ^{210}Pb, and ^{137}Cs) were compared with grain size and organic matter (OM) distributions to assess the factors that influence accumulation of radionuclides. Regression analysis indicated that radionuclide activities were more strongly correlated with OM content than with grain size parameters, and a novel OM-normalisation procedure was developed to correct for preferential nuclide associations. Normalised $^{210}Pb_{xs}$ profiles provide evidence for shifts in sedimentation rates and episodic erosion events in regions of the estuary where anthropogenic disturbance is known to have occurred. Our results emphasise the need to consider radionuclide scavenging by OM in sandy coastal sediments when establishing sedimentation histories.

Additional keywords: Cs-137, estuaries, grain size effect, organic matter, Pb-210, preferential scavenging, radioisotopes, Ra-226.

Introduction

Geochronological techniques that employ atmosphere-derived radionuclides such as ^{210}Pb and ^{137}Cs are frequently used to provide a temporal framework for estuarine sediment deposition that has occurred over the past ~100–150 years (Goldberg *et al.* 1979; Ravichandran *et al.* 1995; Fuller *et al.* 1999). ^{210}Pb can be a particularly useful indicator of sediment accumulation rates and patterns. In chronological applications, the 'excess' component of total measured ^{210}Pb is distinguished from the 'supported' component derived from *in situ* ^{226}Ra decay. Excess ^{210}Pb ($^{210}Pb_{xs}$) is delivered to estuarine waters through several routes, including (1) atmospheric wet or dry deposition, (2) oceanic input, and (3) catchment runoff (Carvalho 1997). It adsorbs rapidly onto particles and their coatings, accumulates on the estuary bottom and decays at a constant rate ($t_{1/2}$ = 22.3 years), providing a tracer of time-dependent sedimentation processes (Oldfield *et al.* 1978). In contrast, the ^{137}Cs-based approach relies on known patterns of atmospheric fallout from nuclear bomb testing that began in 1954 and peaked in 1963. These periods may be identified as stratigraphic peaks in ^{137}Cs activity and provide an independent age marker for corroborating ^{210}Pb-derived ages (Ritchie and McHenry 1990).

Although these techniques assume rapid and non-discriminatory removal of radionuclides from the water column, it has been widely observed that the incorporation of both Pb and Cs radionuclides into sediment is strongly governed by the binding capacity of accumulating particles (Francis and Brinkley 1976; Cremers *et al.* 1988; Loring 1991). Among the physicochemical characteristics that have been related to increased radionuclide binding capacity are: fine-grained texture (Florence and Batley 1980; He and Walling 1996*a*), high smectite or illite clay content (Cremers *et al.* 1988), and high organic matter (OM) content (Nathwani and Phillips 1979; Yeager and Santschi 2003). Preferential nuclide scavenging, often referred to as the 'grain size effect', particularly impacts the distribution of heavy metals in estuaries where a combination of physical processes, including biological mixing, creates complex sediment types (Ackermann 1980; Valette-Silver 1993). As a result, ^{210}Pb depth profiles from dynamic environments often do not exhibit 'ideal' exponential decay profiles or meet the assumptions of Constant Initial Concentration (CIC) or Constant Rate of Supply (CRS) radiometric dating models (Nittrouer *et al.* 1979; Brenner *et al.* 2004). Sediment studies often attempt to minimise these effects by normalising

 10.1071/MF10028 1323-1650/10/111268

radionuclide and metal concentrations to a granulometric or geochemical parameter that reduces the influence of preferential scavenging (Loring 1991). Radiometric applications have traditionally opted for grain size normalizers such as the < 4-μm fraction (Goodbred and Kuehl 1998; Walsh and Nittrouer 2004), whereas heavy metal contamination studies tend to draw from a wider range of normalising phases, including OM content (Kersten and Smedes 2002; Sanders *et al.* 2006).

Given the complicating factors inherent to radiometric studies of dynamic, sand-rich coastal systems, we hypothesise that the effects of preferential scavenging can be quantitatively tested and accounted for in radioisotope data. A primary aim of this study is therefore to investigate these effects in an urbanised estuary, and to explore the efficacy of normalising radioactivity data to a primary carrier phase so that useful information about the sedimentation history may be obtained.

Study area

Naples Bay estuary in south-west Florida (Fig. 1) was targeted to examine the effects of nuclide partitioning on radiometric techniques in dynamic, sandy systems. The estuary is a relatively narrow (20–500 m), shallow (0.5–7.0 m), and microtidal (0.6 m mean tidal range) coastal waterway at the confluence of the Gulf of Mexico, Gordon River, and smaller freshwater tributaries. In the last fifty years, rapid population growth and development has occurred in large portions of the bay's watershed. Typical of many areas along the coast of Florida, dredge and fill operations have transformed the previous shoreline morphology. These actions have destroyed or degraded estuarine habitats, sometimes decimating the fringing mangrove community. Previous studies have indicated that hydrologic factors also contributed to the decline of this ecosystem; freshwater and urban runoff that flows into the bay has increased, and flow and flushing have been impeded by dead-end canal systems (Kreeke 1979; Worley and Hennig 1999). In addition to the conversion of wetlands and mangroves to residential uses, extensive disturbance of freshwater flow followed the construction of the Naples Municipal Airport and the Golden Gate Canal system during the 1950s to 1970s (Surge and Lohmann 2002; Tolley *et al.* 2006; Woithe and Brandt-Williams 2006) by expanding the drainage area of the estuary from 25 to over 300 km^2 (CH2M-Hill 1980) and increasing stormwater discharge into the Gordon River 20- to 40-fold (Simpson *et al.* 1979). These factors contributed to 'slight to moderate' pollution of Naples Bay (Worley and Hennig 1999) and overall decline of water quality (Peterson *et al.* 1984; Surge and Lohmann 2002). Although previous studies have documented regional changes in water quality and ecological response to watershed alteration, an understanding of the sedimentological changes over time is required to identify ecological stresses on biological productivity and establish pre-disturbance conditions for future management of the estuary.

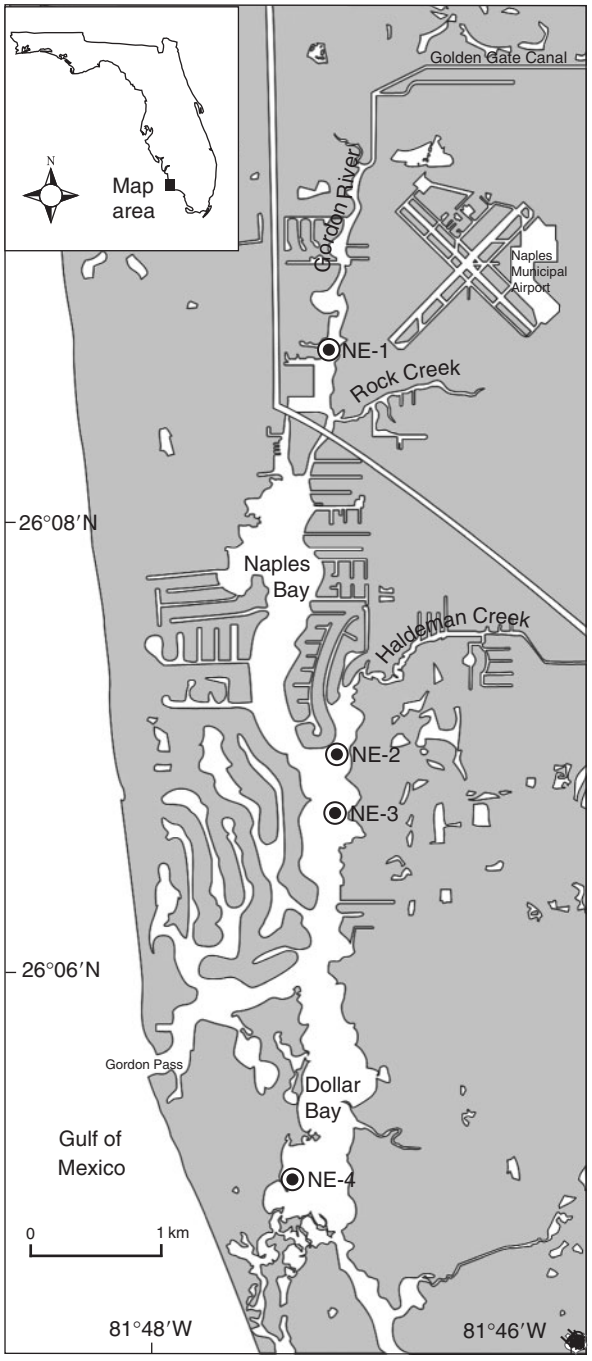

Fig. 1. Locations of cores collected in Naples Bay estuary, Florida.

Materials and methods

Coring and lithological analysis

Sediment cores were collected in April 2005 from four representative regions of the estuary using a 1-m-long, hand-operated piston corer (Fisher *et al.* 1992). Sampling sites (Fig. 1; Table 1) span a range of potential sediment sources and processes from the upper to lower estuary: Gordon River mouth (NE-1), Haldeman Creek mouth (NE-2), mid-Naples Bay (NE-3), and Dollar Bay in the southern arm (NE-4). Coring locations within each region were chosen to be farthest from boat traffic and dredged navigation channels, and in deeper waters as these were most likely to be sediment accumulation sites. Dollar Bay is referred to as a pristine site in this study because it has been relatively unaltered by urban development over the past century.

Table 1. Locations and radiometric characteristics of sediment cores from Naples Bay estuary

Core ID	NE-1	NE-2	NE-3	NE-4
Location	Gordon River	Haldeman Ck	Naples Bay	Dollar Bay
Latitude (N)	26°8′49.0″	26°7′1.0″	26°6′37.0″	26°5′2.5″
Longitude (W)	81°47′9.1″	81°47′5.7″	81°47′6.7″	81°47′19.0″
Core length (cm)	54	34	23	38
$^{210}Pb_{xs}$ inventory	96.7 ± 1.1	35.7 ± 4.5	21.1 ± 3.4	36.7 ± 6.0
Focusing factor[A]	5.4	2.0	1.2	2.1
Penetration depth (cm)	37	28	38	36
SAR_{PEN} (cm year^{-1})[B]	0.3	0.2	0.3	0.3
SAR_{CIC} (cm year^{-1})[C]	n/a	0.3 ± 0.01	n/a	0.4 ± 0.01

[A]Measured inventories of $^{210}Pb_{xs}$ (dpm cm^{-2} $\pm 1\sigma$) were compared with mean atmospheric input to determine a focusing factor at each site. Focusing factor calculation assumes a local atmospherically derived $^{210}Pb_{xs}$ inventory of ~17.9 dpm cm^{-2} from Brenner *et al.* (2001).
[B]SAR_{PEN} gives a whole-core average accumulation rate, assuming penetration depth = 100 y BP, and surface mixed layer thickness = 5 cm.
[C]SAR_{CIC} data were derived for comparison purposes from NE-2 and NE-4, which show three or more consecutive data points with linear correlation coefficients $r^2 > 0.98$ on a natural log scale for activities.

Sediment cores were capped with foam inserts and transported upright to the laboratory where they were split lengthwise and sub-sampled within 48 h. Gamma-ray attenuation was measured at 0.5-cm intervals with a Geotek Multi-Sensor Core Logger (Daventry, UK) and digital images were collected using the GEOSCAN II calibrated colour imaging system (Gunn and Best 1998). A half-round from each core was sectioned at 1- to 3-cm intervals for geochemical analysis and freeze-dried to determine percent dry mass gravimetrically. Depths below the sediment surface were converted to a constant porosity-corrected depth (cm) to minimise the effects of differential compaction according to:

$$\text{Corrected depth} = M_x/((1 - \emptyset)\rho) \quad (1)$$

where M_x = cumulative dry mass (g cm^{-2}); $\emptyset$ = porosity; and ρ = dry density of particles (assumed to be 2.6 g cm^{-3}). This step is essentially equivalent to expressing depth as cumulative dry mass (g cm^{-2}) and gives similar sediment depth profiles (Lu 2007). Weight percentages of sand, silt, and clay were determined on 2- to 4-cm sections of the second half-round using the standard procedures of Douglas and McConchie (1994). Samples were wet-sieved to separate sand (≥63 μm) from fine particles (<63 μm), followed by pipette analysis to determine weight % silt (4–63 μm) and clay (<4 μm) using Stoke's settling velocity calculation.

Bulk geochemical and radiometric analyses

Total sediment OM and $CaCO_3$ contents were determined by loss on ignition (LOI) after Dean (1974). Dried sediment (1–2 g) from each depth interval was weighed in ceramic crucibles and heated in a muffle furnace for 3 h at 550°C to volatilise OM, followed by an additional 3 h at 950°C to oxidise $CaCO_3$. Weight %$CaCO_3$ was calculated assuming complete conversion to CaO. For three of the cores, molar ratios of elemental organic carbon and nitrogen (C : N) were determined using a Carlo Erba NA-1500 CHN Elemental Analyzer (Milan, Italy) via high-temperature Pt-catalysed combustion followed by infrared detection of resulting CO_2 and NO_2 (Verardo *et al.* 1990). Prior to analysis, inorganic carbon was removed using the *in situ* acidification method of Heron *et al.* (1997). In this procedure, samples were acidified directly in the aluminium or silver capsules used for elemental analysis by adding three 100-μL aliquots of 6% sulfurous acid to finely ground sediment, which was dried overnight and re-treated until bubbling ceased. Shell-rich sediment with high $CaCO_3$ content (>20 wt %) often bubbled over or degraded the capsules, thus requiring the use of two nested capsules. Organic carbon determined by elemental analyser correlated well with LOI-derived OM contents (linear correlation coefficient $r^2 = 0.82$; $P < 0.0001$; $n = 64$). However, owing to the complication of removing $CaCO_3$ in carbonate-rich samples, OM data were more readily obtainable and elemental OC values were only used to calculate C : N molar ratios.

Low-background gamma spectroscopy was used to measure the activities of radionuclides ^{210}Pb, ^{226}Ra, and ^{137}Cs according to the methods detailed in Schelske *et al.* (1994). Briefly, dried, ground sediment was packed into 4-mL plastic test tubes, sealed with epoxy and stored for 21 days to minimise loss of short-lived ^{222}Rn gas produced by decay of ^{226}Ra in the sediment matrix. An EG&G Ortec GWL high-purity germanium coaxial-well detector (Oak Ridge, TN) connected to a 4096-channel pulse height-analyser counted radio emissions for ~24 h for each sample, and identified the activities of radioisotopes from their signature emission energies (e.g. 46.5 KeV for ^{210}Pb). Activities of $^{210}Pb_{xs}$ were calculated by subtracting ^{226}Ra from the total ^{210}Pb activity ($^{210}Pb_{tot}$) measured in each sample (Brenner *et al.* 2004). Activity units were in disintegrations per minute (dpm) per gram of sediment and counting errors were calculated by first-order approximation assuming a Poisson distribution of gamma disintegrations (Knoll 1989; Schelske *et al.* 1994). Inventories of $^{210}Pb_{xs}$ activities were calculated as the whole-core sum of incremental activities per unit area of sediment (dpm cm^{-2}), interpolating between measured samples.

Statistical analyses

Relationships between variables were explored using least-squares analysis yielding a linear correlation coefficient (r^2) and significance value (*P*-value) using SigmaPlot software.

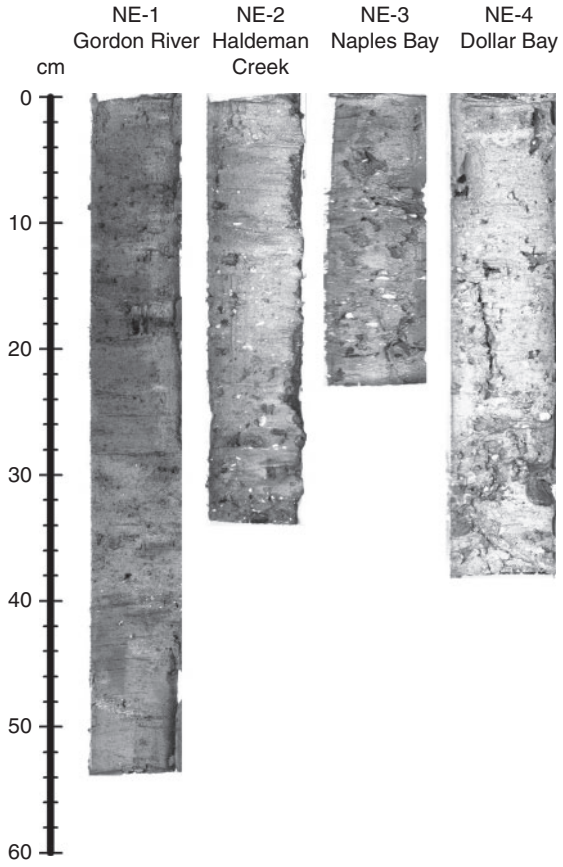

Fig. 2. Digital core images showing variably shell-rich, fines-rich, and sand-rich lithologies, with visibly finer-grained (darker) lenses in NE-1.

Many relationships had significance values just below the more usual $P \leq 0.05$ threshold; we chose to acknowledge these data separately rather than group them with the very poorly correlated relationships. Thus, statistical correlations are reported as $P \leq 0.01$ (very significant), $0.1 \leq P \leq 0.01$ (significant), and $P > 0.1$ (not significant).

Results

Cores ranged in total length from 23 to 54 cm (Table 1) and are depicted in digital images as primarily mottled, sandy muds with abundant oyster shell fragments and thin lenses of fine-grained material (Fig. 2). The sediments are massive to laminated (laminae < 5 mm thick) and marked by biogenic traces and shell horizons typical of estuarine lithofacies. In general, the textural and bulk geochemical profiles show predominantly sandy (>63 μm) sediments with high $CaCO_3$ content (mean $CaCO_3$ > 15 wt %). Each core, however, has distinct textural and compositional features. For example, NE-1 from the mouth of Gordon River is visibly layered and fine-grained in digital photos (Fig. 2). Grain size measurements give a mean value of 42 wt % fines (<63 μm), with stratigraphically variable silt and clay contributions (Fig. 3). This core also displays the greatest range in OM content (5–20 wt %) and organic C : N molar ratios (Fig. 4). C : N vary from 16 to 29, indicating the predominant influence of terrestrially-derived OM (Meyers 1994; Kaushal and Binford 1999). In contrast, C : N ratios from the other core sites only range from 9 to 15, indicating mainly algal and microbial OM sources, with minor terrestrial plant contributions. NE-2 (Haldeman Creek) and NE-4 (Dollar Bay) lack any marked physicochemical variability; fines contents are consistently low (20 ± 5 wt %; ± s.d.), indicating a sandier matrix, whereas OM and $CaCO_3$ contents fall within a similarly consistent range (Fig. 4). NE-3 of mid-Naples Bay shows an overall increase in fine-grained sediment and $\%CaCO_3$ upward in the core. The OM profiles from all cores fail to exhibit a regular decreasing trend with depth that could be attributed to progressive decomposition of labile OM.

Several results can be summarised from the radionuclide activity data (Figs 5 and 6). First, ^{226}Ra remains relatively constant throughout each core, varying ± 0.5 dpm g^{-1} about a mean value of 1.5 dpm g^{-1}, and activities generally do not exceed those of $^{210}Pb_{tot}$ (one exception to this is labelled in Fig. 6 for NE-2). Therefore, it is reasonable to assume that ^{226}Ra–^{210}Pb disequilibrium is not of major concern in Naples Bay estuary, in contrast with some shallow Florida lakes (Brenner *et al.* 2004). Second, $^{210}Pb_{xs}$ shows low initial (surface) activity (<2 dpm g^{-1}) in all but NE-1 (<5 dpm g^{-1}: Fig. 5) and generally exhibits a non-monotonic decrease with depth. A third observation is that, typical of other Florida water bodies (Brenner *et al.* 2004), ^{137}Cs values were very low and did not show a pronounced 1963 peak. Indeed, most values ranged within instrumental error for all cores except NE-1, which exhibited peak ^{137}Cs activity (0.35 ± 0.03 dpm g^{-1}) in the organic-rich layers at 45–50 cm depth, below the maximum depth of $^{210}Pb_{xs}$ (i.e. older than ~100 years).

Discussion

The bulk geochemical and radiometric results provide three principal lines of evidence that point to preferential scavenging effects and non-steady sediment deposition: (1) non-monotonic, down-core decreases in $^{210}Pb_{xs}$ activity profiles in the three upper estuary cores, (2) down-core similarities in the activity profiles of ^{137}Cs and $^{210}Pb_{xs}$ from NE-1, despite contrasting input histories of the two radionuclides, and (3) highly variable $^{210}Pb_{xs}$ inventories. Furthermore, peak ^{137}Cs values at depths below the disappearance of $^{210}Pb_{xs}$ in NE-1 suggest that deposited ^{137}Cs may have diffused out of sandier upper layers into fine-grained, more organic-rich sediment below (Putyrskaya *et al.* 2009).

Low initial radioactivities, in combination with evidence for preferential scavenging, challenge the application of traditional chronological models in sand-rich estuaries, and interpretations are thus less straightforward. We adopted two criteria to provide a context for interpretation of radioisotope profiles from sediment cores: (a) cores must not have been significantly homogenised by syn- or post-depositional mixing (e.g. human dredging operations or intense bioturbation), and (b) cores must come from areas that were zones of sediment accumulation over the lifetime of the radiotracer. NE-1 and NE-3 satisfy the first criterion as they contain textural and chemical stratigraphy (visible layering in NE-1 and steadily increasing $CaCO_3$ content in NE-3) that represent variation in sediment deposition through time, rather than a single, large-scale mixing event. Neither NE-2 nor NE-4, however, contains strong stratigraphic

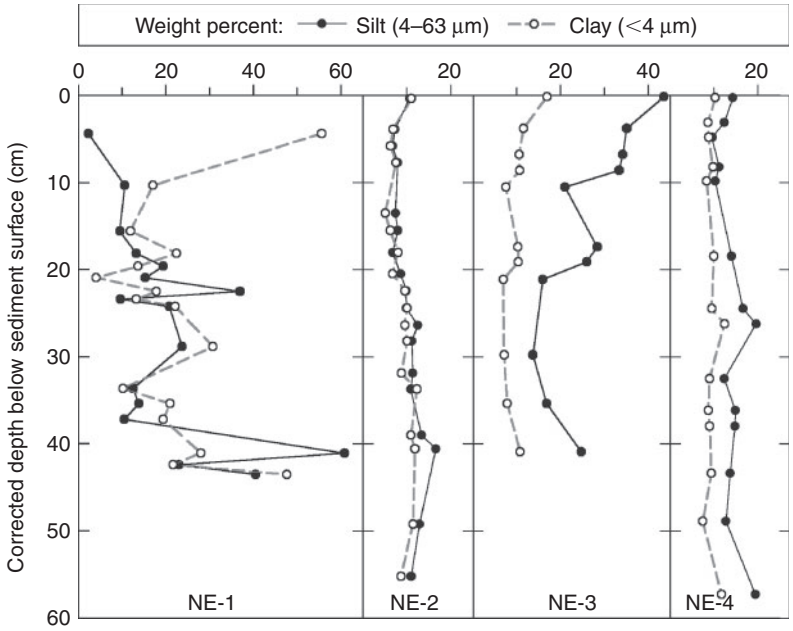

Fig. 3. Percent silt and clay *v.* porosity-corrected depth in sediment.

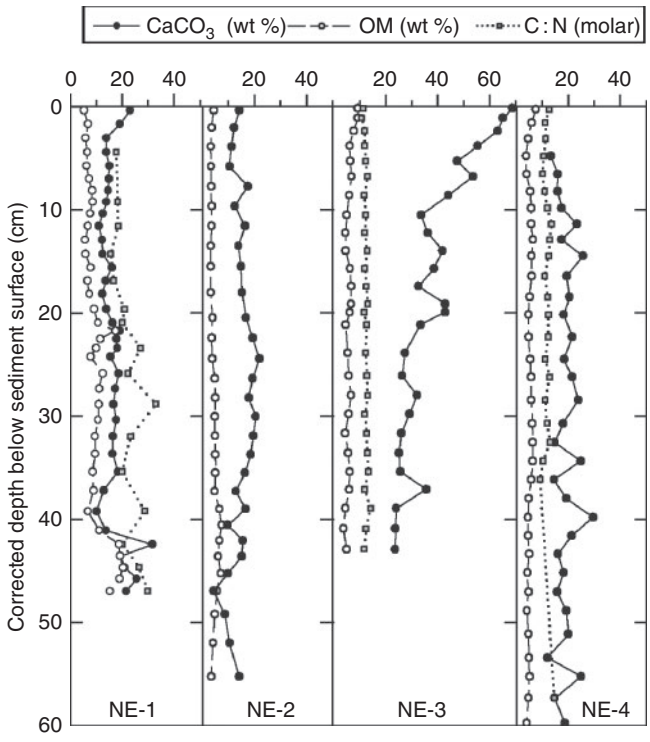

Fig. 4. Profiles of weight percent OM, $CaCO_3$, and molar ratios of organic C : N, plotted *v.* porosity-corrected depth in sediment.

variability in bulk geochemistry and grain size. Therefore, the possibility of mixing must be considered when interpreting the radioactivity profiles from these cores.

One method to test for criterion (b) is to compare the total inventory of $^{210}Pb_{xs}$ activity with fallout inventories measured at nearby locations that have complete depositional records (He and Walling 1996*b*). If inventories from the study site are greater than or equal to reference values, they represent zones of sediment accumulation. Total integrated activities from Naples Bay estuary range widely among the four core sites (21–96 dpm cm^{-2}, Table 1, Fig. 7). In studies of Florida marsh sediments where little sediment import or export occurred, mean $^{210}Pb_{xs}$ fallout rates of 0.6 ± 0.1 dpm cm^{-2} $year^{-1}$ resulted in $^{210}Pb_{xs}$ inventories in the range of 17.9 ± 3.7 dpm cm^{-2} (Brenner *et al.* 2001). The cores collected in Naples Bay estuary therefore represent depositional sites. Furthermore, if the published inventories represent reasonable estimates of the atmospheric fallout component of $^{210}Pb_{xs}$ in the study region, a focusing factor can be calculated as the ratio of measured to reference site inventory. These values, shown in Table 1, reflect the extent to which radionuclide deposition at each site exceeds that expected from atmospheric fallout alone. Focusing factors much greater than 1 for NE-1, NE-2, and NE-4 indicate that material carrying $^{210}Pb_{xs}$ was delivered from other regions of the catchment or estuary. A focusing factor close to 1 for NE-3 could indicate that the $^{210}Pb_{xs}$ at this site is delivered primarily by scavenging from the immediate water column and that there is limited tidal exchange of dissolved excess activity. However, a general correlation between focusing factors and average OM content in each core suggests that preferential scavenging may also account for variation in $^{210}Pb_{xs}$ inventories. Indeed, normalising each $^{210}Pb_{xs}$ inventory to its corresponding total integrated OM content results in $^{210}Pb_{xs}$ inventories that are similar to one another and closer to the local reference values (Fig. 7).

Relationships between radionuclide activity and sediment characteristics

To identify the strongest carrier of radioisotopes in Naples Bay estuary, activities of ^{226}Ra, $^{210}Pb_{tot}$, $^{210}Pb_{xs}$, and ^{137}Cs were compared with wt% of OM, fines, silt, and clay using simple

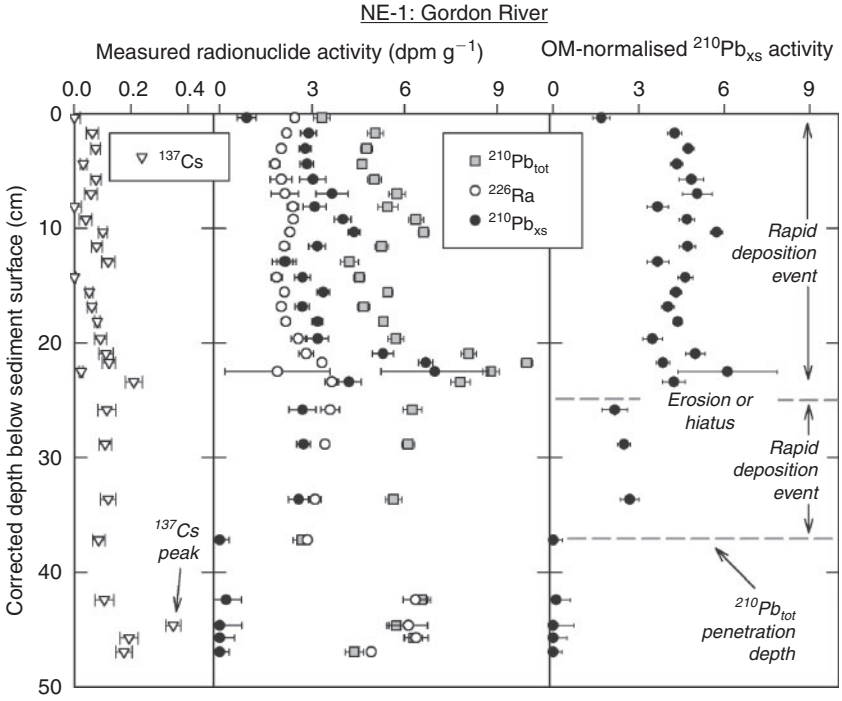

Fig. 5. Radionuclide profiles from NE-1 at the mouth of Gordon River. Left, measured activities of ^{137}Cs, $^{210}Pb_{xs}$, $^{210}Pb_{tot}$, and ^{226}Ra (= supported ^{210}Pb). Right, OM-normalised excess $^{210}Pb_{xs}$ activities. Dashed horizontal lines mark penetration depth and distinguish two rapid depositional events.

linear regression analysis (Table 2). Radionuclide activities were generally positively correlated with OM content, and these relationships were as strong, or stronger than, those between radionuclide activities and any grain size fraction. This relationship occurred despite decay of both the radionuclides and OM over time, which might be expected to reduce the strength of the correlation, unless they disappeared at identical rates. This may be because the portion of OM likely to be resistant to degradation, i.e. humic substances, is also the OM fraction that most efficiently scavenges metals (Stevenson 1994). In NE-2, where the strength of the relationship between ^{226}Ra and grain size was similar to that between ^{226}Ra and OM, a strong correlation was also found between silt and OM content. This indicates that OM is associated with the 4- to 63-μm component of sediment, owing either to preferential OM adsorption to silt-sized particles, or to similar hydrodynamic sorting characteristics.

Organic matter can significantly increase the metal-binding capacity of sediment and is often the primary phase associated with heavy metals in aquatic environments (Foster and Charlesworth 1996; Paulsen *et al.* 1999; Kersten and Smedes 2002). Long water-column residence times, charged functional groups and the ability to make strong multi-dentate bonds may explain the efficiency of both dissolved and particulate OM to scavenge metals from overlying waters and sediment pore waters. Thus, it is not surprising that OM has the potential to be an efficient carrier of heavy metal radionuclides used in sediment dating, such as ^{210}Pb (Yeager and Santschi 2003). Its effect may be particularly important in sandy systems or those of low of clay content. Because bioturbation and bioaccumulation may help incorporate metals into the sediment profile (Yeager *et al.* 2004), the greater macrofaunal density associated with OM-rich sediments may also lead to preferential association of radionuclides with OM-rich layers. Lastly, OM-rich sediments have a greater tendency to become anoxic, which fosters the formation of PbS and other reduced phases that immobilise metals (Benoit and Hemond 1990; Zwolsman *et al.* 1993).

As OM content is readily obtainable, strongly correlated with radionuclide activity, and associated with the <63 μm grain size fractions in this study, it serves as an effective proxy for the range of granulometric and geochemical scavenging processes in Naples Bay estuary. It is thus reasonable to use OM content to mathematically correct radioisotope activities for variability in carrier-phase concentrations through the core.

Radioactivity normalisation

Past sedimentological studies have attempted to correct for the influence of preferential nuclide scavenging by normalising radionuclide activities to various grain size fractions such as clay or fines (Donoghue *et al.* 1998; Goodbred and Kuehl 1998; Grant and Middleton 1998; Clifton *et al.* 1999). We explored the effect of normalising discrete $^{210}Pb_{xs}$ activities to the average OM content in each core to gain insight into the depositional history of the system. OM-normalised activity ($^{210}Pb_{xs\text{-}NORM}$ in dpm g^{-1}) was calculated for each sediment sample at depth z using the equation:

$$^{210}Pb_{xs\text{-}NORM} = {}^{210}Pb_{xs\text{-}MEAS}(OM_{AVG}/OM_z) \qquad (2)$$

where $^{210}Pb_{xs\text{-}MEAS}$ is the measured activity at depth z, and (OM_{AVG}/OM_z) is the ratio of whole-core average OM content to

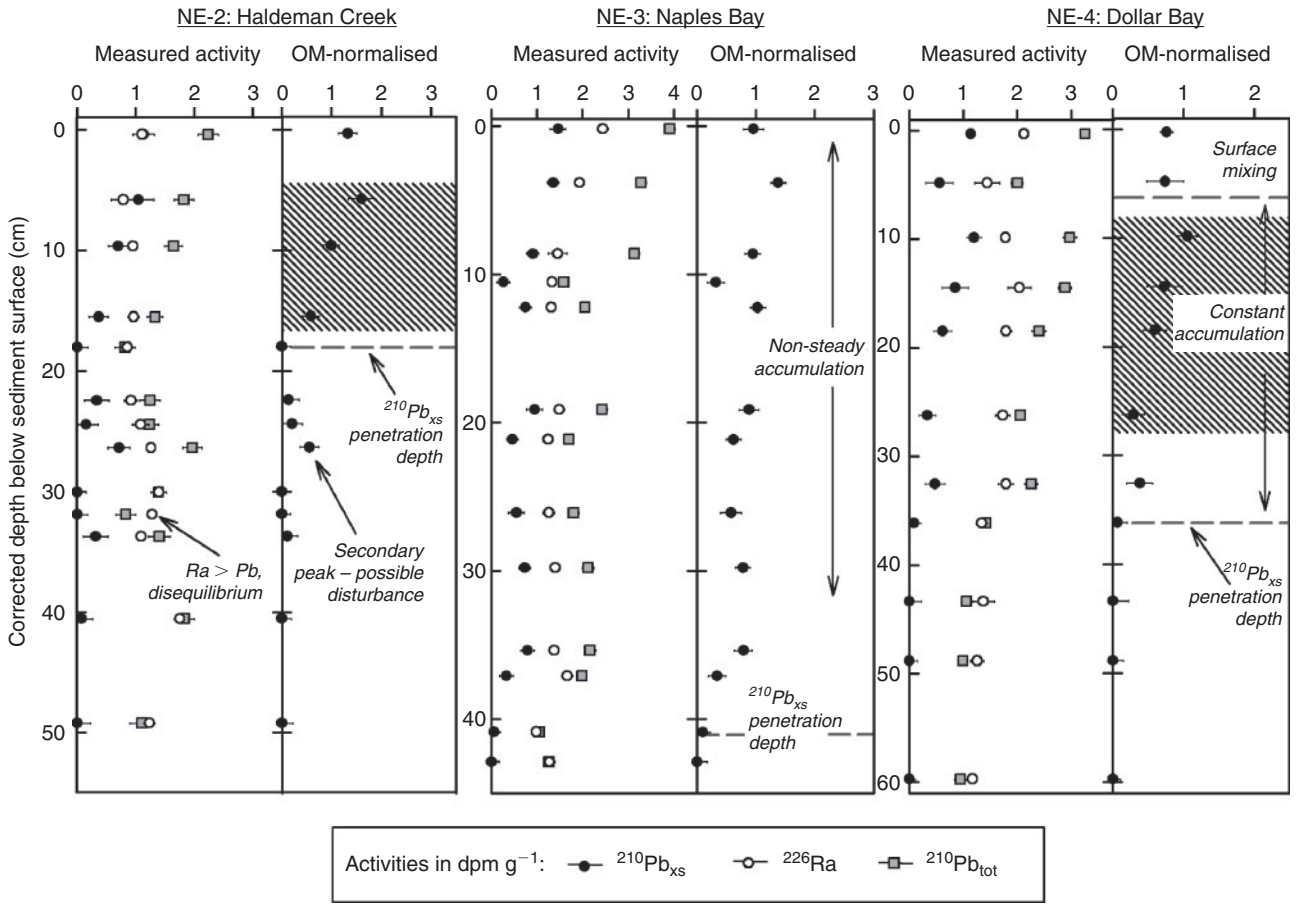

Fig. 6. Radionuclide profiles from NE-2, NE-3, and NE-4. Left of each graph, measured activities of $^{210}Pb_{xs}$, $^{210}Pb_{tot}$, and ^{226}Ra (= supported ^{210}Pb). Right of each graph, OM-normalised $^{210}Pb_{xs}$ activities. Distinct depositional regimes are marked by horizontal dash, and shaded boxes shown in NE-2 and NE-4 indicate data points used for CIC-derived sediment accumulation rates.

OM content of sediment at depth z. Multiplication by this ratio corrects measured activities for variations in OM with respect to an average whole-core value. Compared with the raw activity profiles, OM-normalised $^{210}Pb_{xs}$ profiles (Figs 5 and 6) exhibit reduced scatter and more discernible sediment horizons that can be interpreted as: (1) vertical activity profiles indicating mixed or rapid sediment accumulation, (2) exponentially decreasing $^{210}Pb_{xs}$ activity, indicating constant accumulation rate, and (3) activities within error of 0 dpm g^{-1}, i.e. below the $^{210}Pb_{xs}$ penetration depth, which are interpreted to be more than 100 years old (Nittrouer *et al.* 1979; Walsh and Nittrouer 2004).

Sediment accumulation rate models

Our finding that that OM acts as a preferential carrier phase for ^{210}Pb and ^{226}Ra in Naples Bay estuary calls into question the use of the Constant Initial Concentration (CIC: Robbins 1978) and Constant Rate of Supply (CRS: Appleby and Oldfield 1978) dating models in this system. Although the CRS model has been applied successfully in many sedimentation studies, including some wetland and estuarine environments (Oldfield and Appleby 1984; Brenner *et al.* 2001), it requires that the delivery of $^{210}Pb_{xs}$ activity to the sediment–water interface is constant even if sedimentation rate varies (Binford and Brenner 1986). This means that an increase in sediment supply will dilute the incoming $^{210}Pb_{xs}$ and result in decreased initial activity. However, in Naples Bay estuary, an increase in OM delivery (or other high-binding-capacity components) will increase rather than dilute radionuclide activity, thus invalidating a calculated sedimentation rate by this approach.

The CIC method, in contrast, requires a constant sedimentation rate and a constant initial activity of ^{210}Pb (Robbins 1978). It assumes that an increase in total sediment supply will cause a proportional increase in scavenged ^{210}Pb. This would not be the case in the Naples Bay system where scavenging is controlled more strongly by the variable OM fraction in sediment. Thus, although the CIC model may provide first-order estimates of mean rates of sediment accumulation after removing effects of preferential scavenging of ^{210}Pb by OM, it cannot provide reliable, detailed sedimentation rate data.

Therefore, a conservative approach was employed to determine sediment accumulation rates (SAR) as a whole-core average. The penetration-depth method (Goodbred and Kuehl 1998; Jaeger *et al.* 2009) is based on the assumption that ^{210}Pb decays beyond detectable limits after 4 to 5 half-lives (4.5×22.3 years ≈ 100 years) and uses the maximum penetration depth of $^{210}Pb_{xs}$ (i.e. depth of disappearance) as a marker horizon for

Table 2. Linear correlation coefficients (r^2) for positive relationships between radionuclide activities (dpm g^{-1}), OM content (wt %), and grain size fractions (wt % fines, silt, and clay) for each core

*, $P \leq 0.1$; **, $P \leq 0.01$; ns, $P > 0.1$ (not significant); –, non-relevant relationships or non-detectable activities

Factor	NE-1: Gordon River				NE-2: Haldeman Creek				NE-3: Naples Bay				NE-4: Dollar Bay			
	OM	Fines	Silt	Clay	OM	Fines	Silt	Clay	OM	Fines	Silt	Clay	OM	Fines	Silt	Clay
$^{210}Pb_{tot}$	0.22**	ns	ns	0.40*	ns	ns	ns	ns	0.68**	0.61**	0.63**	0.52*	0.50*	ns	ns	ns
$^{210}Pb_{xs}$	0.48**	0.32*	ns	0.26*	ns	ns	ns	ns	ns	ns	ns	ns	0.35*	ns	ns	ns
^{226}Ra	0.82**	0.31*	0.44*	ns	0.87**	0.76**	0.91**	0.39*	0.79**	0.62**	0.60**	0.62**	0.63**	ns	ns	ns
^{137}Cs	0.49**	ns	ns	ns	–	–	–	–	–	–	–	–	–	–	–	–
Fines	0.22*	–	–	–	0.76**	–	–	–	0.47*	–	–	–	ns	–	–	–
Silt	0.51**	–	–	–	0.81**	–	–	–	0.44*	–	–	–	ns	–	–	–
Clay	ns	–	–	–	0.54**	–	–	–	0.58**	–	–	–	ns	–	–	–

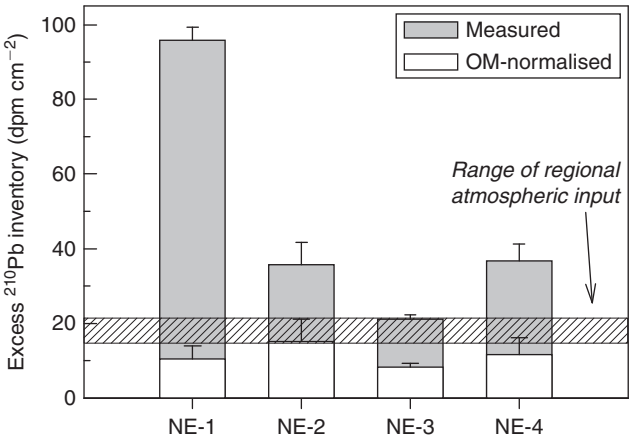

Fig. 7. Measured and OM-normalised values of integrated $^{210}Pb_{xs}$ activity (inventories) compared with those calculated from atmospheric input to other Florida sites.

sediments that are 100 years old. Thus, the 100-year average sedimentation rate does not depend upon assumptions of the CRS or CIC models and can be calculated for each core using:

$$\text{SAR} = (\text{penetration depth} - \text{surface mixed layer})/100 \text{ years} \quad (3)$$

where the surface mixed layer is assumed to be ~5 cm. Results in Table 1 show that accumulation rates are of the order of 0.3 cm year^{-1} except NE-3 from mid-Naples Bay (0.1 cm year^{-1}). Although these are minimum estimates because periods of sediment removal or hiatuses are not accounted for, values are consistent with estimates of relative sea level rise on the Florida coast during the past century (~0.2 cm year^{-1}; Davis 1997).

Interpretation of sedimentation history

OM-normalised $^{210}Pb_{xs}$ activity profiles, $^{210}Pb_{xs}$ inventories and use of the conservative penetration depth approach provide some insight into the temporal and spatial sedimentation trends in the estuary. In NE-1, normalised activities cluster in two groups of near-constant values in the upper ~23 cm and from 23 to 31 cm (Fig. 5). These patterns could indicate homogenisation by macrofaunal mixing. However, evidence of preserved layering in the core suggests that they are more likely to be produced by two discrete mass deposition events, bounded by a hiatus or erosive event. These types of low-frequency, high-energy events that periodically scour the upper estuary sediment beds and then redeposit terrestrial sediment, indicated by high organic C : N ratios, may be related to relatively recent land use changes and channelisation of the watershed.

Below an upper mixed depth of 5 cm, NE-2 from the mouth of Haldeman Creek showed normalised excess activities decreasing steadily down-core until values were within error of zero at 18 cm depth (Fig. 6). Normalisation did not greatly affect this irregular activity profile, probably because OM content was fairly low (~3 wt % mean) and constant throughout the core. Applying the CIC model to the stratigraphic portion containing log-linear, decreasing normalised activity (three data points) yielded a sedimentation rate of 0.3 cm year^{-1}. Although this rate calculation was weakly supported by the data, it is similar to the rate derived by the $^{210}Pb_{xs}$ penetration depth method (0.3 cm year^{-1}, Table 1). Additionally, despite a $^{210}Pb_{xs}$ inventory-derived focusing factor of 2.0, which indicates that the site is a sediment accumulation zone, the lack of apparent physico-chemical stratigraphy limits further insight into the mode of deposition (i.e. constant *v.* non-steady deposition or mixing).

NE-3 from mid-Naples Bay has a $^{210}Pb_{xs}$ profile that is little improved with OM-normalisation, lacking a consistent trend down to the penetration depth of 38 cm (Fig. 6). Stratigraphic increases in $CaCO_3$ and fines content upwards through the core, however, suggest that complete homogenisation did not take place, and the $^{210}Pb_{xs}$ activity profile reflects non-steady deposition rather than mixing. The $^{210}Pb_{xs}$ inventory at NE-3 (21 ± 1.1 dpm cm^{-2}), similar to atmospherically-derived reference inventories, also shows that it was not a sediment- or OM-focusing site. This is reasonable given its location in mid-Naples Bay, a higher-energy environment proximal to heavily used navigation channels and subject to greater wave action from boat traffic and the nearby Gulf of Mexico inlet. The site is also prone to episodic freshwater discharge from the Golden Gate canal system and highly variable sedimentation rates that do not favour constant sediment accumulation.

The activity profile of NE-4, from the more pristine and lower-energy Dollar Bay, shows improved shape after OM-normalisation, displaying a characteristic mixing–accumulation

profile with a surface mixed layer in the upper 5 cm that reflects bioturbation, atop a section of exponentially decreasing $^{210}Pb_{xs}$ from 10 to 30 cm (Fig. 6). Applying the CIC model to this portion of the core yields a sedimentation rate of 0.4 cm year^{-1}, in close agreement with that derived from the $^{210}Pb_{xs}$ penetration depth approach. Despite a relatively constant textural and bulk geochemical stratigraphy, the shape of the $^{210}Pb_{xs}$ profile shows no sign of vertical homogenisation. We therefore interpret this depositional pattern as unmixed and undisturbed over the past century, owing either to its lower-energy setting or to the lack of anthropogenic disturbance in its immediate catchment area compared with the northern arm of the estuary.

Conclusions

The Naples Bay estuary possesses sandy sediments with low radioisotope activities. Therefore, application of traditional chronometric models for dating estuary sediments is not appropriate. Because sediment radionuclide concentrations are strongly associated with OM content, we explored the use of OM-normalised radioactivities to obtain information on sedimentation history. Although only useful in the cores with higher OM contents, OM-normalised radioactivity profiles, in combination with information from $^{210}Pb_{xs}$ penetration depths and inventories, offer insight into bulk sediment accumulation rates and depositional modes at various locations in the estuary over the past 100 years. All core localities record sediment accumulation rates approximately matching sea level rise, and the northern estuary (Naples Bay) is characterised by non-steady sedimentation with greater physical disturbance, including episodes of erosion and rapid deposition. In contrast, the southern estuary (Dollar Bay), where little anthropogenic disturbance has occurred, provides evidence for steady sediment accumulation. We recommend that future work test the application of the OM-normalisation method in other coastal systems to establish a better understanding of the effects of preferential nuclide associations on the depositional record.

Acknowledgements

This research was supported by a grant from The City of Naples to the Conservancy of Southwest Florida. Sincere thanks are extended to Jason Curtis for guidance in the laboratory, to Kathy Worley for field assistance in Naples, and to Michael Macaluso for graphics. We particularly appreciate detailed reviews from Andrew Boulton and anonymous referees, which led to significant improvement of the manuscript.

References

Ackermann, F. (1980). A procedure for correcting the grain-size effect in heavy-metal analysis of estuarine and coastal sediments. *Environmental Technology Letters* **1**, 518–527. doi:10.1080/09593338009384008

Appleby, P. G., and Oldfield, F. (1978). The calculation of Pb-210 dates assuming a constant rate of supply of unsupported Pb-210 to the sediment. *Catena* **5**, 1–8. doi:10.1016/S0341-8162(78)80002-2

Benoit, G., and Hemond, H. F. (1990). Po-210 and Pb-210 remobilization from lake sediments in relation to iron and manganese cycling. *Environmental Science & Technology* **24**, 1224–1234. doi:10.1021/ES00078A010

Binford, M. W., and Brenner, M. (1986). Dilution of Pb-210 by organic sedimentation in lakes of different trophic states and application of studies of sediment water interactions. *Limnology and Oceanography* **31**, 584–595. doi:10.4319/LO.1986.31.3.0584

Brenner, M., Schelske, C. L., and Keenan, L. W. (2001). Historical rates of sediment and nutrient accumulation in marshes of the Upper St. Johns River Basin, Florida, USA. *Journal of Paleolimnology* **26**, 241–257. doi:10.1023/A:1017578330641

Brenner, M., Schelske, C. L., and Kenney, W. F. (2004). Input of dissolved and particulate Ra-226 to lakes and implications for Pb-210 dating of recent sediments. *Journal of Paleolimnology* **32**, 53–66. doi:10.1023/B:JOPL.0000025281.54969.03

CH2M-Hill (1980). The Gordon River watershed study. Big Cypress Basin-South Florida Water Management District. Report No. NA11977 D.O., Naples, Florida.

Carvalho, F. P. (1997). Distribution, cycling and mean residence time of Ra-226, Pb-210 and Po-210 in the Tagus estuary. *The Science of the Total Environment* **196**, 151–161. doi:10.1016/S0048-9697(96)05416-2

Clifton, J., McDonald, P., Plater, A., and Oldfield, F. (1999). Derivation of a grain-size proxy to aid the modelling and prediction of radionuclide activity in salt marshes and mud flats of the eastern Irish Sea. *Estuarine, Coastal and Shelf Science* **48**, 511–518. doi:10.1006/ECSS.1998.0461

Cremers, A., Elsen, A., De Preter, P., and Maes, A. (1988). Quantitative analysis of radiocaesium retention in soils. *Nature* **335**, 247–249. doi:10.1038/335247A0

Davis, R. A. (1997). Regional coastal morphodynamics along the United States Gulf of Mexico. *Journal of Coastal Research* **13**, 595–604.

Dean, W. E. J. (1974). Determination of carbonate and organic matter in calcareous sediments and sedimentary rocks by loss on ignition: comparison with other methods. *Journal of Sedimentary Petrology* **44**, 242–248.

Donoghue, J. F., Ragland, P. C., Chen, Z. Q., and Trimble, C. A. (1998). Standardization of metal concentrations in sediments using regression residuals: an example from a large lake in Florida, USA. *Environmental Geology* **36**, 65–76. doi:10.1007/S002540050321

Douglas, D. W., and McConchie, D. (1994). 'Analytical Sedimentology.' (Chapman and Hall: London.)

Fisher, M. M., Brenner, M., and Reddy, K. R. (1992). A simple, inexpensive piston corer for collecting undisturbed sediment/water interface profiles. *Journal of Paleolimnology* **7**, 157–161. doi:10.1007/BF00196870

Florence, T. M., and Batley, G. E. (1980). Chemical speciation in natural waters. *Critical Reviews in Analytical Chemistry* **9**, 219–296.

Foster, I. D. L., and Charlesworth, S. M. (1996). Heavy metals in the hydrological cycle: trends and explanation. *Hydrological Processes* **10**, 227–261. doi:10.1002/(SICI)1099-1085(199602)10:2<227::AID-HYP357>3.0.CO;2-X

Francis, C. W., and Brinkley, F. S. (1976). Preferential adsorption of Cs-137 to micaceous minerals in contaminated freshwater sediment. *Nature* **260**, 511–513. doi:10.1038/260511A0

Fuller, C. C., van Geen, A., Baskaran, M., and Anima, R. (1999). Sediment chronology in San Francisco Bay, California, defined by ^{210}Pb, ^{234}Th, ^{137}Cs, and $^{239,240}Pu$. *Marine Chemistry* **64**, 7–27. doi:10.1016/S0304-4203(98)00081-4

Goldberg, E. D., Griffin, J. J., Hodge, V., and Koide, M. (1979). Pollution history of the Savannah River estuary. *Environmental Science & Technology* **13**, 588–594. doi:10.1021/ES60153A012

Goodbred, S. L., and Kuehl, S. A. (1998). Floodplain processes in the Bengal Basin and the storage of the Ganges-Brahmaputra River sediment: an accretion study using Cs-137 and Pb-210 geochronology. *Sedimentary Geology* **121**, 239–258. doi:10.1016/S0037-0738(98)00082-7

Grant, A., and Middleton, R. (1998). Contaminants in sediments: using robust regression for grain-size normalization. *Estuaries* **21**, 197–203. doi:10.2307/1352468

Gunn, D. E., and Best, A. I. (1998). A new automated nondestructive system for high resolution multi sensor core logging of open sediment cores. *Geo-Marine Letters* **18**, 70–77. doi:10.1007/S003670050054

He, Q., and Walling, D. E. (1996*a*). Interpreting particle size effects in the adsorption of Cs-137 and unsupported Pb-210 by mineral soils and sediments. *Journal of Environmental Radioactivity* **30**, 117–137. doi:10.1016/0265-931X(96)89275-7

He, Q., and Walling, D. E. (1996*b*). Use of fallout Pb-210 measurements to investigate longer-term rates and patterns of overbank sediment deposition on the floodplains of lowland rivers. *Earth Surface Processes and Landforms* **21**, 141–154. doi:10.1002/(SICI)1096-9837(199602)21:2<141::AID-ESP572>3.0.CO;2-9

Heron, G., Barcelona, M. J., Anderson, M. L., and Christensen, T. H. (1997). Determination of nonvolatile organic carbon in aquifer solids after carbonate removal by sulfurous acid. *Ground Water* **35**, 6–11. doi:10.1111/J.1745-6584.1997.TB00053.X

Jaeger, J. M., Ashish-Mehta, A., Faas, R., and Grella, M. (2009). Anthropogenic impacts on sedimentary sources and processes in a small urbanized subtropical estuary, Florida. *Journal of Coastal Research* **25**, 30–47. doi:10.2112/05-0551.1

Kaushal, S., and Binford, M. W. (1999). Relationship between C : N ratios of lake sediments, organic matter sources, and historical deforestation in Lake Pleasant, Massachusetts, USA. *Journal of Paleolimnology* **22**, 439–442. doi:10.1023/A:1008027028029

Kersten, M., and Smedes, F. (2002). Normalization procedures for sediment contaminants in spatial and temporal trend monitoring. *Journal of Environmental Monitoring* **4**, 109–115. doi:10.1039/B108102K

Knoll, G. E. (1989). 'Radiation Detection and Measurement.' (J. Wiley & Sons: New York.)

Kreeke, J. (1979). Hydrography. In 'The Naples Bay Study'. (Ed. B. L. Simpson.) pp. C1–C6. (The Collier County Conservancy: Naples.)

Loring, D. H. (1991). Normalization of heavy-metal data from estuarine and coastal sediments. *ICES Journal of Marine Science* **48**, 101–115. doi:10.1093/ICESJMS/48.1.101

Lu, X. (2007). A note on removal of the compaction effect for the 210Pb method. *Applied Radiation and Isotopes* **65**, 142–146. doi:10.1016/J.APRADISO.2006.05.010

Meyers, P. A. (1994). Preservation of elemental and isotopic source identification of sedimentary organic matter. *Chemical Geology* **114**, 289–302. doi:10.1016/0009-2541(94)90059-0

Nathwani, J. S., and Phillips, C. R. (1979). Adsorption of Ra-226 by soils. *Chemosphere* **8**, 285–291. doi:10.1016/0045-6535(79)90111-5

Nittrouer, C. A., Sternberg, R. W., Cerpenter, R., and Bennett, J. T. (1979). The use of Pb-210 geochronology as a sedimentological tool: application to the Washington continental shelf. *Marine Geology* **31**, 297–316. doi:10.1016/0025-3227(79)90039-2

Oldfield, F., and Appleby, P. G. (1984). A combined radiometric and mineral magnetic approach to recent geochronology in lakes affected by catchment disturbance and sediment redistribution. *Chemical Geology* **44**, 67–83. doi:10.1016/0009-2541(84)90067-6

Oldfield, F., Appleby, P. G., and Battarbee, R. W. (1978). Alternative Pb-210 dating: Results from the New Guinea Highlands and Lough Ernee. *Nature* **271**, 339–342. doi:10.1038/271339A0

Paulsen, S. C., List, E. J., and Santschi, P. H. (1999). Modeling variability in Pb-210 and sediment fluxes near the Whites Point Outfalls, Palos Verdes Shelf, California. *Environmental Science & Technology* **33**, 3077–3085. doi:10.1021/ES990026U

Peterson, M. E., Yokel, B. J., and Lim, D. V. (1984). Recovery of selected pathogens from Naples Bay, Florida, and associated waterways. *Estuaries* **7**, 133–138. doi:10.2307/1351767

Putyrskaya, V., Eckehard, K., and Röllin, S. (2009). Migration of Cs-137 in tributaries, lake water and sediment of Lago Maggiore (Italy, Switzerland) – analysis and comparison with Lago di Lugano and other lakes. *Journal of Environmental Radioactivity* **100**, 35–48. doi:10.1016/J.JENVRAD.2008.10.005

Ravichandran, M., Baskaran, M., Santschi, P. H., and Bianchi, T. S. (1995). Geochronology of sediments in the Sabine-Neches estuary, Texas, USA. *Chemical Geology. Isotope Geoscience Section* **125**, 291–306.

Ritchie, J. C., and McHenry, J. R. (1990). Application of fallout Cesium-137 for measuring soil erosion and sediment accumulation rates and patterns: a review. *Journal of Environmental Quality* **19**, 215–233. doi:10.2134/JEQ1990.192215X

Robbins, J. A. (1978). Geochemical and geophysical applications of radioactive lead. In 'Biogeochemistry of Lead in the Environment'. (Ed. J. O. Nriagu.) pp. 285–393. (Elsevier Scientific: Amsterdam.)

Sanders, C. J., Santos, I. R., Silva-Filho, E. V., and Patchineelam, S. R. (2006). Mercury flux to estuarine sediments, derived from Pb-210 and Cs-137 geochronologies (Guarantuba Bay, Brazil). *Marine Pollution Bulletin* **52**, 1085–1089. doi:10.1016/J.MARPOLBUL.2006.06.004

Schelske, C. L., Peplow, A., Brenner, M., and Spencer, C. N. (1994). Low-background gamma counting: applications for Pb-210 dating of sediments. *Journal of Paleolimnology* **10**, 115–128. doi:10.1007/BF00682508

Simpson, B. L., Aaron, R., Betz, J., Hicks, D., van der Kreeke, J., *et al.* (1979). The Naples Bay Study. The Collier County Conservancy. Naples, Florida.

Stevenson, F. J. (1994). 'Humus Chemistry: Genesis, Composition, Reactions.' 2nd edn. (John Wiley & Sons: New York.)

Surge, D. M., and Lohmann, K. C. (2002). Temporal and spatial differences in salinity and water chemistry in SW Florida estuaries: effects on human-impacted watersheds. *Estuaries* **25**, 393–408. doi:10.1007/BF02695982

Tolley, S. G., Volety, A. K., Savarese, M., Walls, L. D., Linardich, C., *et al.* (2006). Impacts of salinity and freshwater inflow on oyster-reef communities in Southwest Florida. *Aquatic Living Resources* **19**, 371–387. doi:10.1051/ALR:2007007

Valette-Silver, N. J. (1993). The use of sediment cores to reconstruct historical trends in contamination of estuarine and coastal sediments. *Estuaries* **16**, 577–588. doi:10.2307/1352796

Verardo, D. J., Froelich, P. N., and McIntyre, A. (1990). Determination of organic carbon and nitrogen in marine sediments using the Carlo-Erba NA-1500 Analyzer. *Deep-Sea Research* **37**, 157–165. doi:10.1016/0198-0149(90)90034-S

Walsh, J. P., and Nittrouer, C. A. (2004). Mangrove-bank sedimentation in a mesotidal environment with large sediment supply, Gulf of Papua. *Marine Geology* **208**, 225–248. doi:10.1016/J.MARGEO.2004.04.010

Woithe, D., and Brandt-Williams, S. (2006). Naples Bay surface water improvement and management plan reconnaissance report. South Florida Water Management District, Naples, Florida.

Worley, K., and Hennig, M. (1999). Aqualane Shores – two-year water quality assessment. The Conservancy of Southwest Florida, Naples, Florida.

Yeager, K. M., and Santschi, P. H. (2003). Invariance of isotope ratios of lithogenic radionuclides: more evidence for their use as sediment source tracers. *Journal of Environmental Radioactivity* **69**, 159–176. doi:10.1016/S0265-931X(03)00068-7

Yeager, K. M., Santschi, P. H., and Rowe, G. T. (2004). Sediment accumulation and radionuclide inventories (Pu-239, Pu-240, Pb-210 and Th-234) in the northern Gulf of Mexico, as influenced by organic matter and macrofaunal density. *Marine Chemistry* **91**, 1–14. doi:10.1016/J.MARCHEM.2004.03.016

Zwolsman, J. J. G., Berger, G. W., and Van Eck, G. T. M. (1993). Sediment accumulation rates, historical input, post-depositional mobility and retention of major elements and trace metals in salt marsh sediments of the Scheldt estuary, SW Netherlands. *Marine Chemistry* **44**, 73–94. doi:10.1016/0304-4203(93)90007-B

Manuscript received 6 February 2010, accepted 24 May 2010